symmetry

MDPI

Article

Dispersion of Ultrarelativistic Tardyonic and Tachyonic Wave Packets on Cosmic Scales

José Nicasio and Ulrich D. Jentschura *,†,‡

Department of Physics, Missouri University of Science and Technology, Rolla, MO 65409, USA
* Correspondence: ulj@mst.edu
† Current address: MTA–DE Particle Physics Research Group, P.O. Box 51, H-4001 Debrecen, Hungary.
‡ Current address: MTA Atomki, P.O. Box 51, H-4001 Debrecen, Hungary.

Abstract: We investigate the time propagation of tachyonic (superluminal) and tardyonic (subluminal, ordinary) massive wave packets on cosmic scales. A normalizable wave packet cannot be monochromatic in momentum space and thus acquires a positional uncertainty (or packet width) that increases with travel distance. We investigate the question of how this positional uncertainty affects the uncertainty in the detection time for cosmic radiation on Earth. In the ultrarelativistic limit, we find a unified result, $\delta x(t)/c^3 = m^2 \delta p t / p_0^3$, where $\delta x(t)$ is the positional uncertainty, m is the mass parameter, δp is the initial momentum spread of the wave function, and p_0 is the central momentum of the wave packet, which, in the ultrarelativistic limit, is equal to its energy. This result is valid for tachyons and tardyons; its interpretation is being discussed.

Keywords: symmetry and conservation laws; gauge field theories; gauge bosons

PACS: 11.30.-j; 11.15.-q; 14.70.-e

Citation: Nicasio, J.; Jentschura, U.D. Dispersion of Ultrarelativistic Tardyonic and Tachyonic Wave Packets on Cosmic Scales. *Symmetry* **2022**, *14*, 2596. https://doi.org/10.3390/sym14122596

Academic Editor: Davide Pagano

Received: 15 November 2022
Accepted: 2 December 2022
Published: 8 December 2022

1. Introduction

Aficionados of quantum field theory are interested in the dispersion of ultrarelativistic wave packets on cosmic scales. The unexpected early neutrino burst from the supernova 1987A as reported in [1] still inspires speculations about a potentially tachyonic nature of at least some of the known neutrino species [2]. While this possibility needs to be considered as remote, some interesting conclusions regarding fundamental properties of neutrinos have been derived from the observations [3–5]. The situation gives rise to further questions: Given the dispersion of quantum mechanical wave packets due to the spreading of the momentum-space components, one might speculate that, over very long (cosmic) distance and time scales, the quantum-mechanical wave packet might have spreaded sufficiently to "mimic early arrival" of neutrino bursts, due to position uncertainty after propagation over cosmic scales.

It is well known that, depending on the way in which one interprets the experiments, tiny violations of the causality principle are permissible under the laws of quantum mechanics. Let us consider a wave packet which fulfills the massless one-dimensional Klein–Gordon equation,

$$\phi(t,x) = \frac{1}{(2\pi)^{1/4}\sqrt{\delta x}} \exp\left[-\frac{(x-ct)^2}{4\delta x^2}\right] \cos(x-ct)\,, \qquad \left(\frac{1}{c^2}\frac{\partial^2}{\partial t^2} - \frac{\partial^2}{\partial x^2}\right)\phi(t,x) = 0\,, \tag{1}$$

which is normalized to the condition $\int \mathrm{d}x\, |\phi(t=0,x)|^2 = \int \mathrm{d}x\, |\phi(t,x)|^2 = 1$. The positional uncertainty of the wave packet at time $t = 0$ is easily shown to be equal to $\delta x(t)^2 = \langle x(t)^2\rangle - \langle x(t)\rangle^2 = \delta x^2$ and thus constant in time (no dispersion of the wave packet). Clearly, the wave packet describes an ultrarelativistic spinless particle whose wave function is centered at $\langle x(t)\rangle = c\,t$, but the tip of the wave packet is forward displaced by a

distance δx relative to the center of the wave packet. If the particle were classical, then its trajectory would be described by the expectation value $\langle x(t) \rangle = c\,t$, i.e., the particle would travel on the light cone. However, quantum-mechanically, it is possible for the tip of the wave packet to be ahead by a distance δx. This observation alone, of course, by no means constitutes a violation of causality, but it illustrates the fact that one needs to be careful when analyzing the propagation of quantum mechanical wave packets.

The wave packet given in Equation (1) shows no dispersion over time, or, equivalently, the uncertainty $[\delta x(t)]^2 = \delta x^2$ is constant in time. Ultrarelativistic particles traveling at exactly the speed of light are described by wave packets which do not display dispersion, because all momentum components travel at the speed of light c, and the phase velocity c is equal to the group velocity $\partial E/\partial p = \partial(c\,p)/\partial p = c$. One can understand the dispersion of quantum-mechanical wave packets, in a somewhat colloquial, low-level analogy, by considering a herd of cows: The faster cows will form the tip of the herd, while the slower cows will stay behind. The positional uncertainty $\delta x(t)^2$ of the herd grows with time. The same phenomenon applies to an "ultrarelativistic herd of cows" corresponding to the quantum mechanical wave packet that describes a massive, ultrarelativistic Dirac particle. Here, the dispersion relation is $E = \sqrt{p^2 + m^2}$ (we assume $p = p_x$ to be the momentum in the x direction), and the phase velocity E/p is not equal to the group velocity $\partial E/\partial p = p/E < c$. The dispersion relation $E = \sqrt{p^2 + m^2}$ describes particles traveling at speeds lower than the speed of light (so-called tardyonic particles). Recently, the tachyonic Dirac equation has been studied in detail [6]. As is well known, the dispersion relation for tachyonic particles reads as $E = \sqrt{p^2 - m^2}$. Again, the phase velocity E/p is not equal to the group velocity, yet the group velocity $\partial E/\partial p = p/E > c$ is superluminal.

When we detect ultrarelativistic particles on Earth of cosmic origin, a natural question to ask concerns the spread of the quantum mechanically "allowed" arrival times, assuming that the wave packets describing particles, on their way through cosmos, propagated according to the free tardyonic and tachyonic Dirac equations. Here, we thus engage in the interesting task to study the dispersion of wave packets solving the free tardyonic and tachyonic Dirac equations, and to study the time evolution of the positional uncertainy under the free tardyonic and tachyonic Dirac equations.

This paper is organized as follows: In Section 2, we study the bispinor solutions (in the helicity basis) which constitute the basis of our considerations. In Section 3, we employ an expansion about the central momentum value p_0 of the wave packet in order to evaluate that positional uncertainty of the wave packet as a function of time. The cosmic limit is discussed in Section 4. Conclusions are reserved for Section 5. Natural units with $\hbar = c = \epsilon_0 = 1$ are used everywhere in our calculations unless stated otherwise.

2. Bispinor Solutions

2.1. General Considerations

In order to write the solutions for the tachyonic and tardyonic Dirac equations [6–15],

$$\left(\mathrm{i}\gamma^\mu \partial_\mu - \gamma^5\, m\right) \Psi(x) = 0 \qquad \text{(tachyonic)}\,, \tag{2a}$$

$$\left(\mathrm{i}\gamma^\mu \partial_\mu - m\right) \psi(x) = 0 \qquad \text{(tardyonic)}\,, \tag{2b}$$

we resort to the the helicity basis adapted to the ultrarelativistic case [8]. (Throughout this paper, quantities referring to tachyonic entities such as bispinor wave functions are denoted by uppercase Greek and Latin symbols, while quantities pertaining to tardyonic entities are lowercase. Standard notation is used in Equation (2) for the Dirac gamma matrices γ^μ, the partial derivatives $\partial_\mu \equiv \partial/\partial x^\mu$, the mass parameter m, and the space-time point $x = (t, \vec{r})$.)

In order to meaningfully discuss the dispersion of an ultrarelativistic wave packet, and study quantum propagation, we need to construct normalizable states. It is well known that momentum eigenstates are normalized to a Dirac-δ in momentum space and their wave functions cannot be normalized to unity in coordinate space [15]. This problem has

been considered in various contexts before. An example can be found in photon wave packets, which are interpreted as photon wave functions in Ref. [16]. Specifically, in the discussion surrounding Equation (365) of Ref. [16], Gaussian envelope factors are investigated. Hermite–Gaussian modes (in momentum space) are discussed in Equation (122) of Ref. [17] in order to discuss wave-packet quantization of photons, inspired by previous work [18] in this direction.

Here, we employ the Gaussian envelope function

$$f(p) = \frac{(2\pi)^{1/4}}{\sqrt{\delta p}} \exp\left(-\frac{(p-p_0)^2}{4\delta p^2}\right), \tag{3}$$

which is normalized to unity

$$\int \frac{\mathrm{d}p}{2\pi} |f(p)|^2 = 1, \tag{4}$$

and has the property

$$\langle p^2 \rangle - \langle p \rangle^2 = \delta p^2. \tag{5}$$

The mean-square momentum uncertainty is equal to δp^2.

2.2. Tachyonic Dirac Spinors

The tachyonic bispinor solutions have been studied by us in Refs. [6–9,11,13,14]. We recall the two-component helicity spinors as

$$a_+(\vec{k}) = \begin{pmatrix} \cos\left(\frac{\theta}{2}\right) \\ \sin\left(\frac{\theta}{2}\right) \mathrm{e}^{\mathrm{i}\,\varphi} \end{pmatrix}, \quad a_-(\vec{k}) = \begin{pmatrix} -\sin\left(\frac{\theta}{2}\right) \mathrm{e}^{-\mathrm{i}\,\varphi} \\ \cos\left(\frac{\theta}{2}\right) \end{pmatrix}, \tag{6}$$

where θ and φ are the polar and azimuth angles of the wave vector $\vec{k}$. We start from the negative-helicity, positive-energy solution given in Equations (2.8) and (3.2b) of Ref. [9],

$$\Psi(t,\vec{r}) = \begin{pmatrix} \sqrt{\frac{|\vec{p}|-m}{2\,|\vec{p}|}}\, a_-(\vec{p}) \\ -\sqrt{\frac{|\vec{p}|+m}{2\,|\vec{p}|}}\, a_-(\vec{p}) \end{pmatrix} \exp(-\mathrm{i}E\,t + \mathrm{i}\vec{p}\cdot\vec{r}), \qquad E = \sqrt{\vec{p}^{\,2} - m^2}. \tag{7}$$

For $\vec{p} = p_x \hat{\mathrm{e}}_x = p\hat{\mathrm{e}}_x$, one has $\theta = 90^\circ = \pi/2$ and $\varphi = 0$. Then,

$$\Psi(t,x,p) = \frac{f(p)}{2} \begin{pmatrix} -\sqrt{(p-m)/p} \\ \sqrt{(p-m)/p} \\ \sqrt{(p+m)/p} \\ -\sqrt{(p+m)/p} \end{pmatrix} \exp\left(-\mathrm{i}\sqrt{p^2-m^2}\,t + \mathrm{i}p\,x\right), \qquad |\Psi(t,x,p)|^2 = f(p)^2. \tag{8}$$

A normalizable wave packet is thus obtained as

$$\Psi(t,x) = \int \frac{\mathrm{d}p}{2\pi} \frac{f(p)}{2} \begin{pmatrix} -\sqrt{(p-m)/p} \\ \sqrt{(p-m)/p} \\ \sqrt{(p+m)/p} \\ -\sqrt{(p+m)/p} \end{pmatrix} \exp\left(-\mathrm{i}\sqrt{p^2-m^2}\,t + \mathrm{i}p\,x\right). \tag{9}$$

It is normalized to

$$\int \mathrm{d}x\, |\Psi(t,x)|^2 = \int \mathrm{d}x\, \Psi^+(t,x)\, \Psi(t,x) = \int \frac{\mathrm{d}p}{2\pi} |f(p)|^2 = 1. \tag{10}$$

If one takes the ultrarelativistic limit ($p \gg m$) in the bispinor prefactor, one obtains a somewhat simpler form, which illustrates the connection to the spinless case,

$$\Psi(t,x) \approx \int \frac{\mathrm{d}p}{2\pi} \frac{f(p)}{2}\, \underline{u} \exp\left(-\mathrm{i}\sqrt{p^2-m^2}\, t + \mathrm{i} p\, x\right), \tag{11}$$

where $\underline{u} = (-1,1,1,-1)^{\mathrm{T}}$. Since $f(p)$ is peaked in the region $p \approx p_0 \gg m$, this integration region eventually dominates in all subsequent calculations.

2.3. Tardyonic Dirac Spinors

We start from the negative-helicity, positive-energy solution given in Equations (2.8) and (2.10b) of Ref. [9],

$$\psi(t,\vec{r}) = \begin{pmatrix} \sqrt{\dfrac{E+m}{2\,E}}\; a_-(\vec{p}) \\ -\sqrt{\dfrac{E-m}{2\,E}}\; a_-(\vec{p}) \end{pmatrix} \exp(-\mathrm{i}E\,t + \mathrm{i}\vec{p}\cdot\vec{r}), \qquad E = \sqrt{\vec{p}^{\,2}+m^2}. \tag{12}$$

The solution describing a positive-energy, negative-helicity particle is given as

$$\psi(t,x,p) = \frac{1}{2}\begin{pmatrix} -\sqrt{(E+m)/E} \\ \sqrt{(E+m)/E} \\ \sqrt{(E-m)/E} \\ -\sqrt{(E-m)/E} \end{pmatrix} \exp\left(-\mathrm{i}\sqrt{p^2+m^2}\, t + \mathrm{i} p\, x\right), \qquad |\psi(t,x,p)|^2 = 1. \tag{13}$$

A normalizable wave packet is obtained as

$$\psi(t,x) = \int \frac{\mathrm{d}p}{2\pi} \frac{f(p)}{2} \begin{pmatrix} -\sqrt{(E+m)/E} \\ \sqrt{(E+m)/E} \\ \sqrt{(E-m)/E} \\ -\sqrt{(E-m)/E} \end{pmatrix} \exp(-\mathrm{i}E\,t + \mathrm{i} p\, x). \tag{14}$$

It is normalized to

$$\int \mathrm{d}x\, |\psi(t,x)|^2 = \int \mathrm{d}x\, \psi^+(t,x)\, \psi(t,x) = \int \frac{\mathrm{d}p}{2\pi} |f(p)|^2 = 1. \tag{15}$$

If we take the ultrarelativistic limit ($p \gg m$) in the bispinor prefactor, then we can approximate the solution as

$$\psi(t,x) \approx \int \frac{\mathrm{d}p}{2\pi} \frac{f(p)}{2}\, \underline{u} \exp\left(-\mathrm{i}\sqrt{p^2+m^2}\, t + \mathrm{i} p\, x\right), \tag{16}$$

where $\underline{u} = (-1,1,1,-1)^{\mathrm{T}}$.

3. Standard Wave Packet

3.1. Tachyonic Case

We start from Equation (11). The tachyonic standard wave packet, derived from Equation (11), reads as

$$\Psi(t,x) = \frac{(2\pi)^{1/4}}{\delta p} \int \frac{\mathrm{d}p}{2\pi} \exp\left(-\mathrm{i}\sqrt{p^2-m^2}\, t + \mathrm{i} p\, x - \frac{(p-p_0)^2}{4\delta p^2}\right) \tag{17}$$

It fulfills the (spinless) tachyonic wave equation,

$$\left(\frac{1}{c^2}\frac{\partial^2}{\partial t^2} - \frac{\partial^2}{\partial x^2} + m^2\right) \Psi(t,x) = 0, \tag{18}$$

Its normalization is as follows,

$$\int \mathrm{d}x\, |\Psi(t,x)|^2 = 1\,, \qquad \langle X(t)\rangle = \int \mathrm{d}x\, x\, |\Psi(t,x)|^2\,, \qquad \langle X(t)^2\rangle = \int \mathrm{d}x\, x^2\, |\Psi(t,x)|^2\,. \tag{19}$$

In the calculation of $\langle X(t)\rangle$, one needs to consider three integrals, namely, those over the two momentum parameters defining the wave functions, and one over the x coordinate. With advantages, one calculates the x integral first, with the help of the formula

$$\int \mathrm{d}x\, x\, \exp\bigl(\mathrm{i}(p-p')x\bigr) = -\mathrm{i}\frac{\partial}{\partial p}\delta(p-p')\,. \tag{20}$$

One then differentiates the integrand, and applies the Dirac-δ function, reducing the problem to a one-dimensional p integral with an exponential weight factor. In the last step, one does the remaining p integral under the appropriate ultrarelativistic approximations. The tachyonic expectations values read as follows,

$$\begin{aligned}\langle [X(t)]^2\rangle = {} & \frac{1}{4\delta p^2} + t^2 + \frac{m^2\, t^2}{p_0^2} + \frac{m^4 + 3m^2\delta p^2}{p_0^4}\, t^2 + \frac{10m^4\delta p^2 + 15m^2\delta p^4 + m^6}{p_0^6}\, t^2 \\ & + \frac{m^8 + 21\, m^6\, \delta p^2 + 105\, m^4\, \delta p^4 + 105\, m^2\, \delta p^6}{p_0^8} t^2 + \mathcal{O}(p_0^{-10})\,,\end{aligned} \tag{21}$$

for the position, and

$$\begin{aligned}[\langle X(t)\rangle]^2 = {} & t^2 + \frac{m^2\, t^2}{p_0^2} + \frac{m^4 + 3m^2\delta p^2}{p_0^4}\, t^2 + \frac{9m^4\delta p^2 + 15m^2\delta p^4 + m^6}{p_0^6}\, t^2 \\ & + \frac{m^8 + 18\, m^6\, \delta p^2 + \frac{177}{2}\, m^4\, \delta p^4 + 105\, m^2\, \delta p^6}{p_0^8} t^2 + \mathcal{O}(p_0^{-10})\end{aligned} \tag{22}$$

for its square. The mean-square uncertainty of the position, as a function of time, is found as follows,

$$\delta X(t)^2 = \langle [X(t)^2]\rangle - [\langle X(t)\rangle]^2 = \frac{1}{4\delta p^2} + \frac{m^4\, \delta p^2\, t^2}{p_0^6} + \left(\frac{33m^4\, \delta p^4}{2p_0^8} + \frac{3m^6\, \delta p^2}{p_0^8}\right) t^2 + \mathcal{O}(p_0^{-10}) \tag{23}$$

At $t = 0$, the Heisenberg uncertainty relation is fulfilled in the minimal way, in the sense that $\delta x^2\, \delta p^2 = 1/4$. If one takes the bispinor prefactors from the spin-1/2 solution given in Equation (8) into account, then some additional terms are found for $t = 0$,

$$\begin{aligned}\langle [X(0)^2]\rangle_{s=1/2} - \langle [X(0)^2]\rangle_{s=0} = {} & \frac{m^2}{4p_0^4} + \frac{1}{p_0^6}\left(\frac{5}{2}m^2\delta p^2 + \frac{1}{4}m^4\right) \\ & + \frac{1}{p_0^8}\left(\frac{1}{4}m^6 + \frac{21}{4}m^4\delta p^2 + \frac{105}{4}m^2\delta p^4\right) + \mathcal{O}(p_0^{-10})\,.\end{aligned} \tag{24}$$

This approach leads to formulas for the time-dependent expectation values $\langle X(t)]\rangle$ and $\langle [X(t)^2]\rangle$, but does not discuss the time-dependent form of the wave function itself. An approximate calculation of time propagated wave function can, however, be accomplished as follows. One starts from the representation

$$\Psi(t,x) = \frac{(2\pi)^{1/4}}{\sqrt{\delta p}} \int \frac{\mathrm{d}p}{2\pi} \exp(\mathrm{i}\,\Phi(t,x,p))\,, \qquad \Phi(t,x,p) = -\sqrt{p^2 - m^2}\, t + p\, x + \mathrm{i}\frac{(p-p_0)^2}{4\delta p^2}\,. \tag{25}$$

The dominant momentum region is around $p \approx p_0$. One expands $\Phi(t,x,p)$ about $p = p_0$, up to second order in $(p - p_0)$, and integrates over the resulting Gaussian function in p, after completing the square. The result for the density $|\Psi(t,x)|^2$ is finally found in a relatively compact form,

$$R(t,x) = |\Psi(t,x)|^2 = \mathcal{N}(t,x)\,\exp(-\mathcal{G}(t,x))\,, \qquad \mathcal{N}(t,x) = \sqrt{\frac{2}{\pi}}\,\frac{(p_0^2-m^2)^{3/2}\,\delta p}{\sqrt{(p_0^2-m^2)^3+4m^4t^2\delta p^4}}\,, \tag{26a}$$

$$\mathcal{G}(t,x) = \frac{2(p_0^2-m^2)^2\,\delta p^2}{(p_0^2-m^2)^3+4m^4t^2\delta p^4}\left[p_0^2(t^2+x^2)-m^2x^2-2p_0\sqrt{p_0^2-m^2}\,t\,x\right] \tag{26b}$$

Let us consider an example and temporarily restore SI units. For illustration purposes, we consider

$$m = 10\,\mathrm{u}\,, \qquad p_0 = 100\mathrm{u}\,c\,, \qquad \delta p = 8\mathrm{u}\,c\,, \qquad t_0 = 12\frac{\hbar}{\mathrm{u}c^2}\,, \tag{27}$$

where u is an arbitrarily chosen mass scale, c is the speed of light, and $\hbar$ is Planck's unit of action. These parameters lead to a numerically and graphically convenient representation (see Figure 1, where in the figure, we set $\hbar = \mathrm{u} = c = 1$). Numerically, one obtains the results

$$\sqrt{\langle[X(t_0)]^2\rangle} = 12.061842\frac{\hbar}{\mathrm{u}c}\,, \qquad \langle X(t_0)\rangle = 12.061676\frac{\hbar}{\mathrm{u}c}\,, \qquad \delta\langle[X(t_0)]^2\rangle = 0.0040125\left(\frac{\hbar}{\mathrm{u}c}\right)^2. \tag{28}$$

The first terms listed in Equation (23) add up to

$$\frac{\hbar^2}{4\delta p^2}+\frac{(mc)^4\,\delta p^2\,(ct)^2}{p_0^6}+\left(\frac{33(mc)^4\,\delta p^4}{2p_0^8}+\frac{3(mc)^6\,\delta p^2}{p_0^8}\right)(ct)^2 = 0.0040109\left(\frac{\hbar}{\mathrm{u}c}\right)^2, \tag{29}$$

leading to very good agreement with the analytic result (23). Note that the initial mean-square positional uncertainty is $\delta\langle[X(t=0)]^2\rangle = 0.00390625(\hbar/(\mathrm{u}c))^2$, which is manifestly different from the result given in Equation (28). We now switch back to natural units.

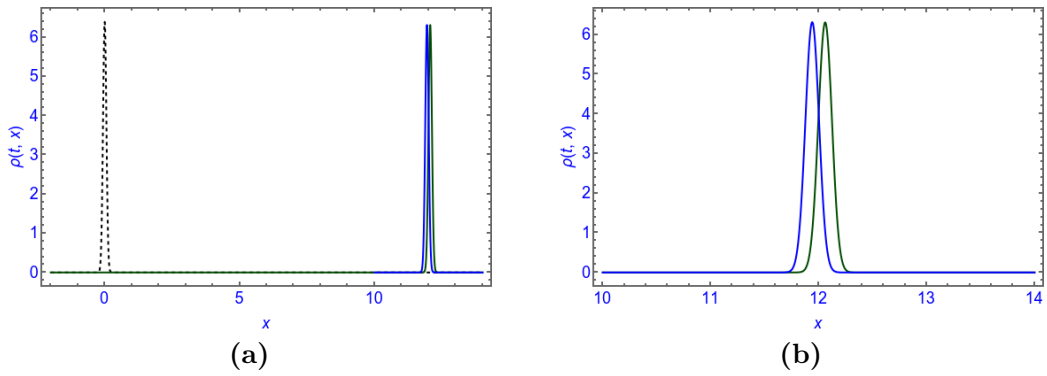

Figure 1. We illustrate the time-propagated tachyonic and tardyonic wave functions for the example case $m = 10$, $p_0 = 100$, $\delta p = 8$, and $t_0 = 12$, given in Equation (27). The dashed curve in (**a**) displays the initial density $\rho(t = 0, x)$, while the blue curve shows the tardyonic density $\rho(t = t_0, x)$ and the dark green curve shows the tachyonic time-evolved function $R(t = t_0, x)$. As demonstrated more clearly in the close-up in (**b**), the tachyonic wave has propagated a little faster in the positive x direction as compared to the tardyonic wave. The positional uncertainty of the time-evolved tachyonic and tardyonic wave packets is almost the same, as is evident from Equations (28), (29), (39), (40) and (42).

3.2. Tardyonic Case

We start from Equation (16) and define a tardyonic standard wave packet,

$$\psi(t,x) = \frac{\sqrt{2\pi}}{\delta p}\int\frac{\mathrm{d}p}{2\pi}\exp\left(-\mathrm{i}\sqrt{p^2+m^2}\,t+\mathrm{i}p\,x-\frac{(p-p_0)^2}{4\delta p^2}\right). \tag{30}$$

It solves the tardyonic (subluminal) wave equation,

$$\left(\frac{1}{c^2}\frac{\partial^2}{\partial t^2} - \frac{\partial^2}{\partial x^2} - m^2\right)\Psi(t,x) = 0\,. \tag{31}$$

The normalization is as follows,

$$\int \mathrm{d}x\,|\Psi(t,x)|^2 = 1\,, \qquad \langle x(t)\rangle = \int \mathrm{d}x\,x\,|\Psi(t,x)|^2\,, \qquad \langle x(t)^2\rangle = \int \mathrm{d}x\,x^2\,|\Psi(t,x)|^2\,. \tag{32}$$

The tardyonic expectation value of the mean-square position is

$$\begin{aligned}\langle [x(t)]^2\rangle = {} & \frac{1}{4\delta p^2} + t^2 - \frac{m^2\,t^2}{p_0^2} + \frac{m^4 - 3m^2\delta p^2}{p_0^4}\,t^2 + \frac{10m^4\delta p^2 - 15m^2\delta p^4 - m^6}{p_0^6}\,t^2 \\ & + \frac{m^8 - 21\,m^6\,\delta p^2 + 105\,m^4\,\delta p^4 - 105\,m^2\,\delta p^6}{p_0^8}t^2 + \mathcal{O}(p_0^{-10})\,.\end{aligned} \tag{33}$$

The square of the expected position is

$$\begin{aligned}[\langle x(t)\rangle]^2 = {} & t^2 - \frac{m^2\,t^2}{p_0^2} + \frac{m^4 - 3m^2\delta p^2}{p_0^4}\,t^2 + \frac{9m^4\delta p^2 - 15m^2\delta p^4 - m^6}{p_0^6}\,t^2 \\ & + \frac{m^8 - 18\,m^6\,\delta p^2 + \frac{177}{2}\,m^4\,\delta p^4 - 105\,m^2\,\delta p^6}{p_0^8}t^2 + \mathcal{O}(p_0^{-10})\end{aligned} \tag{34}$$

The mean-square coordinate uncertainty is thus

$$\delta x(t)^2 = \langle [x(t)^2]\rangle - [\langle x(t)\rangle]^2 = \frac{1}{4\delta p^2} + \frac{m^4\,\delta p^2\,t^2}{p_0^6} + \left(\frac{33m^4\,\delta p^4}{2p_0^8} - \frac{3m^6\,\delta p^2}{p_0^8}\right)t^2 + \mathcal{O}(p_0^{-10})\,, \tag{35}$$

which is seen to be equivalent to the result given in Equation (23) upon the replacement $m \to \mathrm{i}\,m$. One finds, for the solution in Equation (13), additional terms at the initial time $t = 0$,

$$\begin{aligned}\langle [x(0)^2]\rangle_{s=1/2} - \langle [x(0)^2]\rangle_{s=0} = {} & \frac{m^2}{4p_0^4} + \frac{1}{p_0^6}\left(\frac{5}{2}m^2\delta p^2 - \frac{1}{2}m^4\right) \\ & + \frac{1}{p_0^8}\left(\frac{3}{4}m^6 - \frac{21}{2}m^4\delta p^2 + \frac{105}{4}m^2\delta p^4\right) + \mathcal{O}(p_0^{-10})\,.\end{aligned} \tag{36}$$

For the approximate calculation of time-propagated wave function, one employs the same steps that lead to Equation (26) in the tachyonic case. One writes the wave function as

$$\psi(t,x) = \frac{\sqrt{2\pi}}{\delta p}\int \frac{\mathrm{d}p}{2\pi}\exp(\mathrm{i}\phi(t,x,p))\,, \qquad \phi(t,x,p) = -\sqrt{p^2+m^2}\,t + p\,x + \mathrm{i}\frac{(p-p_0)^2}{4\delta p^2}\,. \tag{37}$$

Then, one expands $\phi(t,x,p)$ about $p = 0$, up to second order in $(p = p_0)$, and integrates over the resulting Gaussian function in p, after completing the square. The result is

$$\rho(t,x) = |\psi(t,x)|^2 = n(t,x)\,\exp(-g(t,x))\,, \qquad n(t,x) = \sqrt{\frac{2}{\pi}}\,\frac{(p_0^2+m^2)^{3/2}\,\delta p}{\sqrt{(p_0^2+m^2)^3 + 4m^4t^2\delta p^4}}\,, \tag{38a}$$

$$g(t,x) = \frac{2(p_0^2+m^2)^2\,\delta p^2}{(p_0^2+m^2)^3 + 4m^4t^2\delta p^4}\left[p_0^2(t^2+x^2) + m^2x^2 - 2p_0\sqrt{p_0^2+m^2}\,t\,x\right]. \tag{38b}$$

We consider the same example as in Equation (27), $m = 10\,\mathrm{u}$, $p_0 = 100\,\mathrm{u}\,c$, $\delta p = 8\,\mathrm{u}\,c$, and $t_0 = 12\hbar/(\mathrm{u}c^2)$, but for the tardyonic case, and temporarily switch to SI units (again). Numerically, one obtains the results

$$\sqrt{\langle [X(t_0)]^2 \rangle} = 11.939453 \frac{\hbar}{\mathrm{u}c}, \qquad \langle X(t_0) \rangle = 11.939286 \frac{\hbar}{\mathrm{u}c}, \qquad \delta \langle [X(t_0)]^2 \rangle = 0.0040058 \left(\frac{\hbar}{\mathrm{u}c} \right)^2. \tag{39}$$

The first terms listed in Equation (35) add up to

$$\frac{\hbar^2}{4\delta p^2} + \frac{(mc)^4\, \delta p^2\, (ct)^2}{p_0^6} + \left(\frac{33\,(mc)^4\, \delta p^4}{2 p_0^8} + \frac{3\,(mc)^6\, \delta p^2}{p_0^8} \right) (ct)^2 = 0.0040054 \left(\frac{\hbar}{\mathrm{u}c} \right)^2. \tag{40}$$

This result is in very good agreement with the analytic result (35). A plot which illustrates the difference between tachyonic and tardyonic propagation is found in Figure 1 (where we set $\hbar = \mathrm{u} = c = 1$ in the plot). From now on, we again switch to natural units.

4. Cosmic Limit

Up to this point, we have assumed that p_0 is the largest variable in the problem. The cosmic limit is obtained when one considers large propagation times and distances. It is appropriate to scale $t \to \lambda\, t$ and $x \to \lambda\, x$ and to keep only the leading-order terms in λ. A careful investigation of the expressions for $R(t, x)$ and $\rho(t, x)$ is sufficient. One can, in fact, integrate over x and x^2 with the densities given in Equations (26) and (38), and calculate the standard deviation of the position expectation value. The limit of large t, small m, and large p_0 is obtained as

$$\delta X(t)^2 \approx \delta x(t)^2 \approx \frac{m^4\, \delta p^2\, t^2}{p_0^6}, \qquad t \to \infty. \qquad \frac{\delta p}{p_0} \ll 1, \qquad \frac{m}{p_0} \ll 1. \tag{41}$$

In order to confirm and ramify the result, one observes that the limit of large t, and $m \ll \delta p \ll p_0$ means that the $1/p_0^8$ terms in Equations (23) and (35) are suppressed in comparison to the $1/p_0^6$ term, which is listed in Equation (41). Finally, since we are investigating the ultrarelativistic limit, it is useful to convert the positional uncertainty into a detection time uncertainty acquired for the detection of the ultrarelativistic particle coming in from the cosmos, and convert the result to SI mksA units. We choose as the cosmic travel time an interval of 168,000 light years, which is the distance to the Large Magellanic Could, where the supernova 1987A originated [1]. One finds

$$\left. \frac{\delta X(t)}{c} \right|_{t=168{,}000\,\mathrm{yr}} \approx \left. \frac{\delta x(t)}{c} \right|_{t=168{,}000\,\mathrm{yr}} \approx 5.298 \times 10^{-6}\, \frac{\delta \xi}{\xi} \left(\frac{\chi}{\xi} \right)^2 \mathrm{s}, \tag{42}$$

where "s" of course is the symbol for the unit "second", $\delta\xi$ is the momentum spread in GeV/c, ξ is equal to the central momentum p_0 in GeV/c, and χ is the mass of the particle, measured in eV/c^2. It means that, if the particle wave function is centered about a well-defined ultrarelativistic mean momentum $p_0 \gg m$ (i.e., $\delta\xi/\xi \ll 1$ and $\chi/\xi \ll 1$), then the detection time uncertainty amounts to less than a microsecond even for cosmic travel over appreciable distances (here, as an example, the distance to the Large Magellanic Cloud). The result (42) applies equally to tachyons as well as tardyons.

5. Conclusions

In this paper, we have investigated the propagation of ultrarelativistic tachyonic and tardyonic wave packets on short as well as cosmic time and distance scales. In Section 2, we study the positive-energy bispinor solutions of left helicity of the tachyonic and tardyonic Dirac equations, which describe propagation in the positive x direction of an ultrarelativistic spin-1/2 particle. We use these as exemplary states in order to study the problem at hand. Our choice is inspired by the fact that neutrinos, which remain a possible candidate for tachyons, typically occur in left-helicity states. For an up-to-date summary of possible empirical indications that some neutrinos are tachyons, see Ref. [19]. We find that, in the ultrarelativistic limit, the spin-1/2 solution, in the helicity basis, reduces to the spinless so-

lution, multiplied by a constant four-components bispinor (see Equations (11), (16) and (17), as well as (30)).

A normalizable, localizable wave packet of Gaussian shape is used as an initial condition for the time propagation (see Section 3. We find that the mean-square positional uncertainty of the wave packet increases quadratically with time, for both tachyonic as well as tardyonic particles. Our results (for the spinless case) are summarized in Equations (23) and (35). For spin-1/2 particles, the result is (somewhat surprisingly) almost the same, but the initial value (at $t = 0$) for the mean-square positional uncertainty receives a modification according to Equations (24) and (36).

In the cosmic, ultrarelativistic limit ($m \ll p_0$), the time t is the dominant variable, and we assume that the momentum uncertainty δp is also much smaller than p_0. In this limit, the result for the time evolution of the positional uncertainty reduces to a single term, given in Equation (41). This result is proportional to m^4, where m is the mass term, and hence invariant under the replacement $m \to \mathrm{i}\, m$. A numerical evaluation of the result given in Equation (41) reveals that, under reasonable assumptions about the momentum spread of ultrarelativistic particles, the dispersion of ultrarelativistic wave packets is sufficiently small, even on cosmic times scales, that it remains possible to associate the generation time of the particle with the detection time, up to an uncertainty which increases by no more than a microsecond per light year (see Equation (42)). One of the consequences of this result is that the "early" arrival of the neutrino burst under the Mont Blanc, recorded in coincidence with the 1987A supernova, cannot be explained by the positional uncertainty of the propagated ultrarelativistic wave packet on its way from the Large Magellanic Cloud. (Other possible explanations (e.g., Ref. [20]) have been discussed in the literature.) Our result (42) is generally applicable for tachyons and tardyons.

Finally, let us explore if we can understand the result (42) intuitively, with respect to the "herd of cows analogy" made in Section 1. In a wave packet composed of a tardyonic herd, in view of the classical dispersion relation $E = m/\sqrt{1 - v^2}$ (with $v < 1$), the faster "cows" are the ones with more energy. In a tachyonic herd, in view of the classical dispersion relation $E = m/\sqrt{v^2 - 1}$ (with $v > 1$), the faster "cows" are the ones with less energy. In both cases, the herd is composed of faster and slower ones, and the wave packet spreads. This consideration qualitatively explains the universal character of the result (42) for tachyons and tardyons.

Author Contributions: Conceptualization, U.D.J.; formal analysis, J.N. and U.D.J.; investigation, J.N. and U.D.J.; visualization, J.N. and U.D.J. All authors have read and agreed to the published version of the manuscript.

Funding: This research was funded by National Science Foundation grant number PHY-2110294.

Data Availability Statement: Not applicable.

Acknowledgments: The authors acknowledge helpful conversations with José Crespo López–Urrutia on general aspects regarding tachyons.

Conflicts of Interest: The authors declare no conflict of interest.

References

1. Dadykin, V.L.; Zatsepin, G.T.; Karchagin, V.B.; Korchagin, P.V.; Mal'gin, S.A.; Ryazhskaya, O.G.; Ryasnyi, V.G.; Talochkin, V.P.; Khalchukov, F.F.; Yakushev, V.F.; et al. Detection of a rare event on 23 February 1987 by the neutrino radiation detector under Mont Blanc. *JETP Lett.* **1987**, *45*, 593–595.
2. Ehrlich, R. Evidence for two neutrino mass eigenstates from SN 1987A and the possibility of superluminal neutrinos. *Astropart. Phys.* **2012**, *35*, 625–628. [CrossRef]
3. Barbiellini, G.; Cocconi, G. Electric charge of the neutrinos from SN1987A. *Nature* **1987**, *329*, 21–22. [CrossRef]
4. Arnett, W.D.; Rosner, J.L. Neutrino Mass Limits from SN1987A. *Phys. Rev. Lett.* **1987**, *58*, 1906–1909. [CrossRef] [PubMed]
5. Longo, M.J. New Precision Tests of the Einstein Equivalence Principle from SN1987A. *Phys. Rev. Lett.* **1988**, *60*, 173–175. [CrossRef] [PubMed]
6. Jentschura, U.D.; Wundt, B.J. Pseudo–Hermitian Quantum Dynamics of Tachyonic Spin–1/2 Particles. *J. Phys. A* **2012**, *45*, 444017. [CrossRef]

7. Chodos, A.; Hauser, A.I.; Kostelecký, V.A. The Neutrino as a Tachyon. *Phys. Lett. B* **1985**, *150*, 431–435. [CrossRef]
8. Jentschura, U.D.; Wundt, B.J. Localizability of tachyonic particles and neutrinoless double beta decay. *Eur. Phys. J. C* **2012**, *72*, 1894. [CrossRef]
9. Jentschura, U.D.; Wundt, B.J. From Generalized Dirac Equations to a Candidate for Dark Energy. *ISRN High Energy Phys.* **2013**, *2013*, 374612. [CrossRef]
10. Jentschura, U.D.; Horváth, D.; Nagy, S.; Nándori, I.; Trócsányi, Z.; Ujvári, B. Weighing the Neutrino. *Int. J. Mod. Phys. E* **2014**, *23*, 1450004. [CrossRef]
11. Noble, J.H.; Jentschura, U.D. Ultrarelativistic Decoupling Transformation for Generalized Dirac Equations. *Phys. Rev. A* **2015**, *92*, 012101. [CrossRef]
12. Jentschura, U.D.; Ehrlich, R. Lepton-pair Cerenkov radiation emitted by tachyonic neutrinos: Lorentz-covariant approach and Ice Cube data. *Adv. High Energy Phys.* **2016**, *2016*, 4764981. [CrossRef]
13. Jentschura, U.D.; Nándori, I.; Ehrlich, R. Calculation of the decay rate of tachyonic neutrinos against charged-lepton-pair and neutrino-pair Cerenkov radiation. *J. Phys. G* **2017**, *44*, 105201. [CrossRef]
14. Somogyi, G.; Nándori, I.; Jentschura, U.D. Neutrino Splitting for Lorentz–Violating Neutrinos: Detailed Analysis. *Phys. Rev. D* **2019**, *100*, 035036. [CrossRef]
15. Jentschura, U.D.; Adkins, G.S. *Quantum Electrodynamics: Atoms, Lasers and Gravity*; World Scientific: Singapore, 2022.
16. Mohr, P.J. Solutions of the Maxwell equations and photon wave functions. *Ann. Phys.* **2010**, *325*, 607–663. [CrossRef]
17. Smith, B.J.; Raymer, M.G. Photon wave functions, wave-packet quantization of light, and coherence theory. *New J. Phys.* **2007**, *9*, 414. [CrossRef]
18. Kogelnik, H.; Li, T. Laser beams and resonators. *Appl. Opt.* **1966**, *5*, 1550. [CrossRef]
19. Ehrlich, R. A Review of Searches for Evidence of Tachyons. *Symmetry* **2022**, *14*, 1198. [CrossRef]
20. Ehrlich, R. The Mont Blanc neutrinos from SN 1987A: Could they have been monochromatic (8 MeV) tachyons with $m^2 = -0.38\,\mathrm{keV}^2$? *Astropart. Phys.* **2018**, *99*, 21–29. [CrossRef]